CHARACTERIZATION OF EXTENSIVE CITY-SCALE SOLAR POWER GENERATION

REPORT 2017:388





Characterization of extensive city-scale solar power generation

Findings from the UppScaleSolar project

JOAKIM WIDÉN, GUSTAV ELFVING, EMIL JANSSON, JOAKIM MUNKHAMMAR, DAVID LINGFORS

Foreword

This is a project conducted within the program SOLEL which runs as a cooperation between the Swedish Energy Agency and the industry. It was initiated in order to provide knowledge about ways to host large amounts of PV-electricity in urban areas.

When the share of electricity generated from sun increases, is there also a larger need to adjust production after consumption. Knowledge about how this can be managed efficiently is interesting for a variety of stakeholders, from spatial planners to grid owners.

The project was managed by Uppsala University with Joakim Widén as project manager.



Sammanfattning

Antalet nätanslutna solcellssystem i världen har ökat snabbt de senaste decennierna, vilket antyder att framtidens städer inte bara kommer att vara lastcentra utan stora nettoleverantörer av elkraft. Med höga andelar solel i kraftsystemet kommer utmaningar för både distributions- och transmissionssystemoperatörer. Lokalt kan den momentana totala effekten från utspridda solcellssystem orsaka spänningshöjningar, massivt omvänt effektflöde och överbelastning av komponenter. Snabb effektbalansering inom timmen och behovet av förstärkning av transmissionsnätet påverkas av graden av variabilitet i framtida solkraft och dess geografiska utbredning.

I det här projektet har vi studerat variabilitet i solkraft över en geografisk skala om 1-10 km, vilket motsvarar utbredningen för en medelstor svensk stad. Projektets syfte har varit att utveckla metoder för att kvantifiera variabiliteten hos aggregerad solelproduktion från byggnadsapplicerade solcellssystem (BAPV) på stadsnivå. Framtida solelproduktion i Uppsala, Sverige, analyseras i scenarier baserade på kommunens angivna mål för solel om 30 MW installerad effekt år 2020 och 100 MW år 2030. Modellerna som har utvecklats i projektet används för att karakterisera den totala solelproduktionen i staden vad gäller genomsnittlig dygns- och säsongsvariation, sannolikhet för olika momentana produktionsnivåer och fluktuationer i effekt över olika tidshorisonter.

Ett sensornätverk för solinstrålning konstruerades i Uppsala och användes för att samla in ett års 5-minutersvärden för solinstrålning från 24 solmätare monterade vid 13 olika solcellssystem. Statistiska modeller för solinstrålning anpassades till dessa data och användes tillsammans med simuleringsmodeller för solcellssystem för att karakterisera aggregerad solkraftproduktion på stadsnivå. Modellen för momentan solstrålning som har utvecklats i projektet kan generera tillförlitliga solinstrålningsdata för godtyckliga uppsättningar av geografiskt utspridda solcellssystem.

Fallstudien för Uppsala stad omfattar en kartläggning av tillgängliga områden för BAPV-system med hjälp av s.k. LiDAR-data, vilket ger ett mycket detaljerat underlag för simuleringarna. Simuleringsresultaten visar att den relativa variabiliteten i den sammanlagda solinstrålningen över hela staden är kraftigt utjämnad jämfört med instrålningen på en enskild plats, med en lägre sannolikhet för höga effekter och effektfluktuationer inom timmen. Till exempel är sannolikheten för höga effekttoppar i instrålningen 50-60% lägre i de flesta väder jämfört med instrålningen på en enskild plats.

Data, modeller och resultat från projektet kan användas av kommuner och andra organisationer i energiplanering och vid framtagning av solbruksplaner, av distributions- och transmissionssystemoperatörer vid planering och drift av elnät med höga andelar solkraft. Inte minst kan de också utnyttjas i prognoser av solstrålning och solkraft, där utjämningseffekten som beror på den rumsliga utspridningen är direkt relaterad till prognosens noggrannhet. Alla dessa tillämpningar är intressanta för framtida forskning och utveckling.



Summary

Grid-connected, building-applied solar power has increased rapidly worldwide over the last decades, suggesting that the cities of the future might not just be load centers but major power providers. With large amounts of solar power in the power system, there will be challenges for both distribution and transmission system operators. Locally, the instantaneous aggregate power from dispersed photovoltaic (PV) systems may cause voltage rise, massive reverse power flows and overloading of components. Intra-hourly balancing and the need for capacity in the transmission system will be affected by the degree of variability in future solar power and its geographical distribution.

In this project we have studied solar power variability on a geographic scale of 1-10 km, which is the spatial extent of a medium-sized Swedish city. The aim of the project has been to develop methodologies for quantifying the variability of aggregate solar power generation from building-applied photovoltaic (BAPV) systems in a city and apply these to characterize city-wide solar power generation. The city of Uppsala, Sweden, is analyzed in scenarios based on the city's stated target of 30 MW installed PV power by 2020 and 100 MW by 2030. The models developed in the project are used to characterize the aggregate solar power generation in the city in terms of average daily and seasonal variation, probability for different instantaneous production levels, and fluctuations in power over different time horizons.

A sensor network for solar irradiance was constructed in Uppsala and has collected one year of 5-min solar irradiance data from 24 solar loggers at 13 dispersed PV systems. Based on this data, it was possible to fit statistical models of solar irradiance and use PV system modeling to accurately characterize the aggregate solar power generation of a city. The model for instantaneous solar irradiance developed in the project can generate highly accurate solar irradiance data for any set of building-applied PV systems.

The case study for the city of Uppsala includes a mapping of available areas for BAPV systems using LiDAR (Light Detection And Ranging) data, providing very detailed data for the simulations. In particular the simulated instantaneous irradiance and irradiance step-changes show that there is a considerable smoothing effect on the city-wide aggregate solar power, substantially reducing the probability for high aggregate powers and intra-hourly power fluctuations. For example, over the whole city, the probability for high irradiance peaks (clear-sky index > 1) is reduced by 50-60% in most weathers compared to a single site.

The data, models and findings from the project can be used by municipalities and other organizations in their energy planning and preparation of solar roadmaps, by distribution and transmission system operators for planning and operation of power distribution and transmission networks with high shares of solar power, and not least for forecasting of solar irradiance and solar power, where the smoothing effect resulting from spatial dispersion is directly related to the accuracy of the forecast. All of these applications are interesting for future research and development.



List of content

1	Intro	duction		7
	1.1	Aim a	nd goals of the project	7
	1.2	List of	scientific publications from the project	8
		1.2.1	Peer-reviewed journal papers	8
		1.2.2	Conference papers	g
		1.2.3	PhD theses	g
		1.2.4	Master theses	g
	1.3	Struct	cure of the report	g
2	Meth	ods		10
	2.1	Solar i	irradiance	10
		2.1.1	Solar irradiance logger network	10
		2.1.2	Probabilistic solar irradiance models	13
	2.2	Photo	ovoltaic systems	15
		2.2.1	Photovoltaic system monitoring	15
		2.2.2	Photovoltaic system modeling	16
	2.3	Buildi	ngs	17
		2.3.1	Building surface identification and modeling	17
		2.3.2	Scenarios	19
3	Resu	lts		22
	3.1	Photo	ovoltaic system performance	22
	3.2	Mode	el fitting and validation	22
		3.2.1	Correlation model	22
		3.2.2	Probabilistic solar irradiance model	24
		3.2.3	Photovoltaic system model	26
	3.3	Chara	cterization of city-scale solar power variability	27
		3.3.1	Seasonal and diurnal variability	27
		3.3.2	Instantaneous power generation	29
		3.3.3	Intra-hourly power fluctuations	33
4	Conc	luding d	liscussion	35
Refe	rences			37



1 Introduction

Grid-connected solar power has increased rapidly around the world over the last decades. Considering that a large share of the installed capacity consists of building-applied photovoltaic systems, it is likely that the cities of the future will be big power producers. This report quantifies what we can expect of the city as a solar power plant, using state-of-theart mathematical modeling and a city-wide solar irradiance sensor network.

With large amounts of renewable electricity in the power system, the need for power system reserves to balance changes in net power demand on different time scales will increase depending on the mix of renewables [1,2]. Although trading in the electricity spot market takes place on an hourly basis, transmission system operators (Svenska Kraftnät in Sweden) must manage imbalances on significantly shorter time scales. This intra-hourly balancing (primary, secondary and tertiary control) will be affected by the degree of variability in future solar power. Locally, distribution system operators will also face challenges with high penetrations of solar power, where the instantaneous aggregate power from a whole fleet of photovoltaic (PV) systems may cause voltage rise, massive reverse power flows and overloading of components [3,4].

Variability in renewable power sources is an expanding and fast-moving research area. In a recently published review article, Widén et al. [2] summarized the findings of more than 200 studies on solar, wind, wave and tidal power variability, with emphasis on research from the last few years. An important conclusion was that more effort should be put on quantifying the so-called dispersion-smoothing effect. For a PV system, the output power can change rapidly if a cloud moves over the system, but over a large number of dispersed systems the weather conditions vary so that the aggregate power fluctuations even out. An important question for solar power integration is how high this smoothing effect is in different types of weather and depending on dispersion of systems.

In this project we have studied solar power variability on a geographic scale of 1-10 km, which is the spatial extent of a medium-sized Swedish city. The results show how high smoothing of the aggregate power can be expected in scenarios where solar power is concentrated to buildings within a city.

1.1 AIM AND GOALS OF THE PROJECT

The aim of the project has been to develop methodologies for quantifying the variability of aggregate solar power generation from building-applied photovoltaic (BAPV) systems in a city and apply these to characterize city-wide solar power generation. The project has used Uppsala municipality as a case study, but the methodology is generally applicable and parts of the results are expected to be generally valid for cities of the same size.



The final goal of the project has been to characterize the power output of aggregate solar power production in the city of Uppsala in different future BAPV scenarios. These scenarios are based on Uppsala municipality's stated target of 30 MW installed PV power by 2020 and 100 MW by 2030. The characterization includes quantification of:

- (a) Average daily and seasonal variation.
- (b) The probability for different instantaneous production levels.
- (c) The probability for fluctuations in power output on different time horizons.

A number of concrete milestones for the project have been:

- 1. Collect and evaluate at least one year of high-resolution data for solar irradiance from a monitoring network consisting of at least 13 dispersed PV systems equipped with solar irradiance loggers, and use these data to evaluate PV system performance.
- 2. Develop a model for calculating the output power from an arbitrarily oriented PV system based on high-resolution solar irradiance data. The calculated power output from the model should deviate from the aggregate generation of the systems in the monitoring network by a maximum of 5% on average.
- 3. Develop mathematical models that can describe instantaneous solar irradiance and irradiance variability over a large number of arbitrarily distributed sites in a city. The models should be able to quantify the aggregated power output according to points (a) (c) above.
- 4. Construct scenarios for future expansion of BAPV systems on buildings in Uppsala city, which correspond to the 2020 and 2030 goals of the municipality, and calculate and characterize solar power generation from these systems with the models in milestones 2 and 3.

1.2 LIST OF SCIENTIFIC PUBLICATIONS FROM THE PROJECT

The research project has resulted in a number of scientific publications, already published or in progress, which go into more detail on parts of the findings in this report.

1.2.1 Peer-reviewed journal papers

Joakim Munkhammar, Joakim Widén, "Correlation modeling of instantaneous solar irradiance with applications to solar engineering", Solar Energy 133 (2016) 14-23.

Joakim Munkhammar, Joakim Widén, Laura M. Hinkelman, "A copula method for simulating correlated instantaneous solar irradiance in spatial networks", Solar Energy 143 (2017) 10-21.

Joakim Widén, Mahmoud Shepero, Joakim Munkhammar, "On the properties of aggregate clear-sky index distributions and an improved model for spatially



correlated instantaneous solar irradiance", manuscript submitted to Solar Energy (2017).

1.2.2 Conference papers

Joakim Munkhammar, Jesper Rydén, Joakim Widén, David Lingfors, "Simulating dispersed photovoltaic power generation using a bimodal mixture model of the clear-sky index", Proceedings of the 30th European Photovoltaic Solar Energy Conference (EU PVSEC), Hamburg, Germany, September 14-18, 2015.

Joakim Munkhammar, Joakim Widén, "Copula correlation modeling of aggregate solar irradiance in spatial networks", Proceedings of the 6th International Workshop on Integration of Solar Power into Power Systems, Vienna, Austria, November 14-15, 2016.

1.2.3 PhD theses

David Lingfors, Solar Variability Assessment and Grid Integration: Methodology Development and Case Studies, Licentiate thesis, Department of Engineering Sciences, Uppsala University, 2015.

1.2.4 Master theses

Emil Jansson, Gustav Elfving, Modelling and Evaluation of extensive solar power production in urban and rural areas (prel. title), Master thesis, Department of Engineering Sciences, Uppsala University, 2017.

1.3 STRUCTURE OF THE REPORT

The report is structured as follows. In Section 2 the methods developed and/or applied within the project are described, divided on methods for solar irradiance, PV systems and buildings, including the studied BAPV scenarios. In Section 3 the results of the project are presented, including monitored PV system performance, validation of irradiance and PV system models and characterization of city-scale solar power generation in the scenarios for Uppsala. A concluding discussion in Section 4 summarizes the most important findings from the project.



2 Methods

2.1 SOLAR IRRADIANCE

2.1.1 Solar irradiance logger network

To provide data on dispersed solar irradiance over the city of Uppsala, a monitoring network was constructed using solar irradiance loggers. The requirements on the network sensors were that they should be low-cost, portable and allow logging data with a high enough time resolution (minute-scale). To begin with, experiments were made with solar loggers built in-house [5], but for long-term outdoor reliability reasons the final choice fell on the commercial HOBO Pendant Temperature/Light Data Logger [6], see Figure 1. The logger is calibrated for measuring light levels, but utilizes a linear relationship between irradiance and light and can therefore be recalibrated to measure irradiance.



Figure 1. HOBO Pendant loggers used in the solar irradiance sensor network. Photos: Joakim Munkhammar.

The loggers were set to sample the solar irradiance every 5th minute. This sampling frequency was chosen as a compromise between high time resolution and utilization of the limited memory capability of the loggers (64 kB). With this setting, the loggers were able to store data over one year in their built-in memory cards. Since the loggers cannot be perfectly synchronized, all data were resampled to the same nearest 5-minute interval midpoint. Thus, instantaneous irradiance is measured, but with a 5-minute time accuracy. Still, it is accurate enough for the analyses within the project.

A total of 24 loggers were installed at 13 different sites to measure either global horizontal irradiance (5 loggers) or global irradiance in the module plane (19



loggers). Depending on the system configuration the loggers were mounted at one or several different sub-arrays of the PV system. All measurements took place between March 2016 and March 2017, with all loggers covering the one-year period 24 March 2016 – 23 March 2017. In addition to mounting and taking down the loggers at the beginning and end of the period, the loggers were checked half-way into the measurement period, including a battery change and collection of data. Figure 2 shows a map of the network sites and Table 1 lists the loggers along with their azimuth and tilt angles.

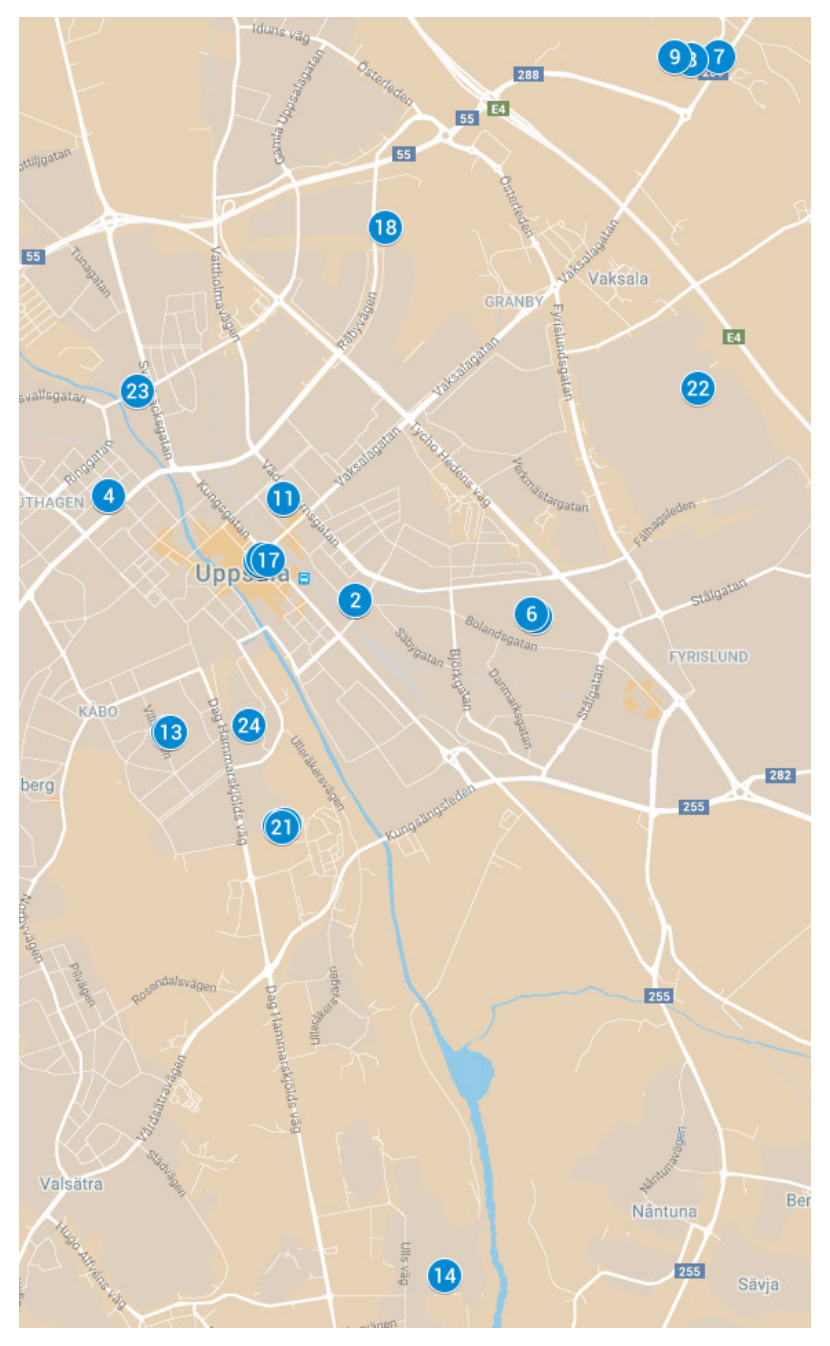


Figure 2. Sites in the solar irradiance sensor network in Uppsala. Numbers are the same as in Table 1.



Table 1. Solar irradiance loggers in the sensor network in Uppsala. Numbers are the same as in Figure 2.

#	Site	Orientation	Azimuth	Tilt	Latitude	Longitude
1	Frodeparken	Horizontal	0	0	59.856885	17.652723
2	Frodeparken	Module plane	- 7	90	59.856885	17.652723
3	Granegården	Horizontal	0	0	59.863409	17.622135
4	Granegården	Module plane east	42	26	59.863409	17.622135
5	Bolandsgatan	Horizontal	0	0	59.855832	17.675355
6	Bolandsgatan	Module plane	-16	8	59.855945	17.674786
7	Vaksala Eke	Tracker	-	-	59.890848	17.698138
8	Vaksala Eke	Horizontal/roof	0	0	59.890718	17.694726
9	Vaksala Eke	Module plane facade	15	90	59.890891	17.692688
10	Salagatan	Horizontal	0	0	59.863248	17.643819
11	Salagatan	Module plane	42	30	59.863248	17.643819
12	Geocentrum	Module plane west	67	15	59.848544	17.629476
13	Geocentrum	Module plane south	-23	20	59.848532	17.629849
14	Ultuna	Module plane	0	39	59.814466	17.663885
15	Sala	Module plane C	-45	5	59.859254	17.640993
16	Sala	Module plane D	-45	8	59.859397	17.641342
17	Sala	Module plane E	45	25	59.859355	17.641943
18	Gränby ishall	Module plane	- 5	14	59.880236	17.656588
19	SciencePark	Module plane west	80	10	59.842694	17.643343
20	SciencePark	Module plane east	-100	10	59.842783	17.644078
21	SciencePark	Module plane south	-10	10	59.842641	17.643759
22	Ångelsta	Module plane	-30	20	59.870133	17.695622
23	Fyrishov	Module plane	-19	90	59.869985	17.625643
24	Akademiska Sjukhuset	Module plane	15	3	59.849000	17.639628

In some of the analyses it is necessary to normalize the solar irradiance data in order to remove all systematic diurnal and seasonal variability due to the sun's position in the sky. This was done using clear-sky irradiance data for the same dates and times from the McClear model [7]. The so-called clear-sky index was calculated as

$$\kappa = \frac{G}{G_c} \tag{1}$$

where G is the measured solar irradiance and G_c is the modelled clear-sky irradiance in the same plane. To parameterize the irradiance models to depend on the daily level of cloudiness, the daily clear-sky index is also used, defined as

$$\bar{\kappa} = \frac{\int G}{\int G_c} \tag{2}$$



where the integrals are evaluated between sunrise and sunset. For non-horizontal irradiance, the in-plane clear-sky irradiance was calculated from global and diffuse clear-sky irradiance components using standard transposition formulae for the tilted plane (see Section 2.2.2 below).

To compare and complement the data collected in Uppsala, irradiance data from a much denser sensor network at Oahu Island, Hawaii, was used [8]. That network consists of 17 pyranometers measuring global horizontal irradiance on a 1-second basis over station separations up to roughly 1 km. This data is described in more detail in the scientific papers [9,10].

In addition to this, hourly data for a median year between 1999-2014, based on solar irradiance data from SMHI's database STRÅNG [11], was used to be able to model future city-wide solar power in the scenarios for Uppsala.

2.1.2 Probabilistic solar irradiance models

Within the project, statistical models were developed and used to determine probability distributions for instantaneous solar irradiance and irradiance fluctuations over different time horizons. Both of these models depend on the assumed correlation between dispersed sites, for which a model was formulated and fitted to the solar irradiance data. All of these models are described below.

Correlation model

Based on observations of the solar irradiance data for Hawaii it was hypothesized that the correlation between instantaneous irradiance data at two sites first decreases rapidly with increasing site separation (up to around 1 km), and then levels out for larger separations (above 1 km). To model this behavior an exponential decay model with two exponential terms was formulated (previously suggested by [12]):

$$\rho_{\kappa}(d) = \beta e^{-\alpha_1 d} + (1 - \beta) e^{-\alpha_2 d} \tag{3}$$

where ρ is the correlation, d is the distance between two sites, β defines the relative proportions of the two exponential functions and α_1 and α_2 determine how fast the correlation decreases with distance.

Model for instantaneous irradiance

The probabilistic model for instantaneous solar irradiance treats the clear-sky index at an individual site as a stochastic variable with a certain probability distribution. As hypothesized by Hollands and Suehrcke [13], this distribution has three peaks, corresponding to three states of the atmosphere: clear skies, overcast skies and broken cloud cover. In our model, we separate the clear state and the two cloudy states into two stochastic variables, so that the clear-sky index can be expressed as

$$\kappa = S\kappa_{\text{clear}} + (1 - S)\kappa_{\text{cloudy}} \tag{4}$$

where *S* is a stochastic variable that is either 1 or 0 and indicates clear or cloudy weather. Thus, *S* has a so-called Bernoulli distribution



$$S \sim \text{Bernoulli}(s)$$
 (5)

with *s* being the probability for clear weather. In the clear state the clear-sky index is modelled by a Gaussian distribution

$$\kappa_{\text{clear}} \sim N(\mu_s, \sigma_s^2)$$
 (6)

with mean value μ_s and standard deviation σ_s . In the cloudy state the clear-sky index is modelled with a Gaussian mixture model having a probability density function that is a sum of two Gaussian density functions:

$$p(\kappa) = \sum_{i=1}^{2} w_i f_N(\kappa | \mu_i, \sigma_i^2)$$
 (7)

where w_1 and w_2 are the weights of the two Gaussian functions corresponding to overcast and broken cloud states, respectively, f_N is the Gaussian density function, and μ_1 , μ_2 and σ_1 , σ_2 are mean values and standard deviations.

Probability distributions for the aggregate clear-sky index over an arbitrary set of sites are calculated using a Monte Carlo approach in which correlated uniform random numbers are generated with a Gaussian copula. The covariance matrix of the copula has values for each site pair given by the correlation function in Equation 3. The correlated random numbers are then fed through the inverse of the cumulative distribution function for κ to yield samples of the clear-sky index at each site that are correlated according to their dispersion. A more detailed description of the procedure for generating correlated samples from clear-sky index distributions is given in [10].

Model for irradiance fluctuations

Irradiance power fluctuations, also called step-changes, are defined, based on the clear-sky index, as

$$\Delta \kappa(t) = \kappa(t) - \kappa(t - 1) \tag{8}$$

where t denotes the time step in a time series with some resolution. To characterize the smoothing effect that geographical dispersion has on the step-changes, a commonly used measure is the relative variability [14] $\sigma \tau^2/\sigma^2$, which is the ratio between the variance of the aggregate clear-sky index over a set of sites and the variance of the clear-sky index at one individual site.

To model the relative variability over a set of arbitrary sites the method proposed by Widén [14] is used. In this method, dispersion is analyzed in the time domain, since distances between sites can be defined by the time it takes for a cloud to move between them, given a constant cloud speed. Thus, the distance d between two sites can be expressed in the time domain as

$$\tau = -\frac{d}{v}\cos\varphi \tag{9}$$

where v is the cloud speed and ϕ is the angle between the cloud motion vector and the axis defined by the two sites. The correlations between step-changes can now be calculated from the correlations between instantaneous values as



$$\rho_{\Delta\kappa}(\tau) = \frac{2\rho_{\kappa}(\tau) - \rho_{\kappa}(\tau - \bar{t}) - \rho_{\kappa}(\tau + \bar{t})}{2(\rho_{\kappa}(0) - \rho_{\kappa}(\bar{t}))} \tag{10}$$

where \bar{t} is the averaging time of the data series. From these correlations between sites, the relative variability can be determined as

$$\frac{\sigma_T^2}{\sigma^2} = \frac{1}{N^2} \sum_i \sum_j \rho_{\Delta\kappa}(\tau_{ij}) \tag{11}$$

where N is the total number of sites and τ_{ij} is the time-domain separation between a pair of sites.

Additional irradiance models developed in the project

Besides the models described above, the project has also resulted in a number of other scientifically important findings and models. We showed that an accurate model for global irradiance at an individual site can be formulated based on separate probabilistic modeling of the beam and diffuse components, connected by a copula that models the negative correlation between the two components [18]. In this model, the instantaneous global clear-sky index is a stochastic variable:

$$X = X_d + X_b \tag{12}$$

where X_d and X_b are stochastic variables representing diffuse and beam components, assumed to be Gamma and Bernouilli distributed, respectively. This formulation of the global clear-sky index as a sum of the two components directly leads to an Ångström-type [19] equation for the expected solar irradiance:

$$\frac{H}{H_c} = \gamma \delta + \beta p \tag{13}$$

where H and H_c are expected values for global and global clear-sky irradiation (total irradiation over a long period of time), γ and δ are parameters defining the Gamma distribution, β is a scaling factor for the Bernoulli distribution, and p is the probability for bright sunshine (beam radiation > 0). This is usually written as

$$\frac{H}{H_c} = a + bS \tag{14}$$

where a and b are the so-called Ångström coefficients and S is the fraction of bright sunshine (i.e., S = p). This means, for example, that probabilistic models can be formulated (assuming a relation between γ and δ) based only on Ångström coefficients, which are available for many locations around the world [20]. Deeper investigations into how beam and diffuse irradiance and Ångström coefficients relate to the three-state model for instantaneous irradiance described above can lead to further model improvement.

2.2 PHOTOVOLTAIC SYSTEMS

2.2.1 Photovoltaic system monitoring

In addition to logging irradiance at the PV systems, production data for the systems was collected in order to validate the PV system model and evaluate



system performance. For these data we had to rely on the already existing monitoring and logging systems at each site. For this reason, the data quality, time period covered and time resolution differ considerably between systems. Table 2 gives an overview of the data that were available for each system. As can be seen, neither production data nor irradiance could be collected for all subsystems. This means that evaluation of system performance and model validation in many cases could not be done for the complete systems.

Table 2. PV systems from which production data could be obtained.

Site	Owner	Installed power (kW)	Time reso- lution	Subsystems with production data	Subsystems with irradiance data
Frodeparken	Uppsalahem	100	Day	6/12	1/12
Granegården	BRF Granegården	39	Hour	3/3	1/3
Bolandsgatan	Industrihus	47	Day	3/3	1/3
Vaksala Eke (facade)	Industrihus	11	15 min	1/1	1/1
Salagatan	Industrihus	10	Day	2/3	1/3
Geocentrum	Akademiska hus	45	Month	3/3	2/3
Ultuna	Akademiska hus	6.3	Hour	1/2	2/2
Sala	Vasakronan	75	Hour	6/6	3/6
SciencePark	Vasakronan	58	Day	4/4	3/4

2.2.2 Photovoltaic system modeling

The PV system model was developed in order to have a simple yet accurate method for determining PV yield that could be smoothly integrated with the building area identification and keep the computational complexity of the whole process down. The model converts beam and diffuse radiation components on the horizontal plane to AC power output from the inverter in a number of steps. The first step is to determine the irradiance that is absorbed in the solar cells. This is done using the following model, which includes a transposition of the radiation components to the tilted plane of the PV modules and a calculation of absorbed irradiance:

$$G_{T} = k_{b}G_{b}R_{b} + G_{d}\left(k_{d}(1 - A_{i})\left(\frac{1 + \cos\beta}{2}\right) + k_{b}A_{i}R_{b}\right) + k_{g}(G_{b} + G_{d})\rho_{g}\left(\frac{1 - \cos\beta}{2}\right)$$
(15)

where G_b and G_d are beam and diffuse radiation on the horizontal plane, respectively, R_b is a scaling factor for beam radiation based on the incidence angles of the radiation on the tilted and horizontal planes, A_i is the anisotropy index, which is the fraction of extraterrestrial radiation preserved as beam radiation, β is the tilt angle of the tilted plane, ρ_g is the albedo of the ground, and the factors k_b , k_d and k_g are incidence angle modifiers (IAM) accounting for reflection losses determined with the Sandia IAM model [15].



The absorbed radiation heats up the solar cells, which in turn affects the efficiency of the modules. To account for this the cell temperature is determined as

$$T_c = T_a + G_T \left(\frac{T_{c,NOCT} - 20}{800} \right) (1 - \eta_0)$$
 (16)

where T_a is the ambient temperature, $T_{c,NOCT}$ is the nominal operating cell temperature (NOCT) obtained at 20°C ambient temperature and 800 W/m² irradiance, and η_0 is the module efficiency at standard test conditions (STC), 25°C cell temperature and 1000 W/m² irradiance. The efficiency of the PV modules can then be determined as

$$\eta = \eta_0 (1 + \Delta P_T (T_c - 25)) \tag{17}$$

where ΔP_T is the temperature coefficient of the maximum power (percentual change in power, and thus efficiency per degree change in cell temperature).

The DC power output of the whole PV array is

$$P_{dc} = NAG_T \eta (1 - l_a) \tag{18}$$

where N is the number of modules, A is the individual module area and l_a is the percentage of additional losses, e.g., soiling, mismatch losses, etc. The AC power output of the inverter is determined using the Sandia inverter model [16]:

$$P_{ac} = C_0 (P_{dc} - P_{s0})^2 + C_1 (P_{dc} - P_{s0})$$
(19)

where P_{s0} is the threshold power of the inverter and C_0 and C_1 are parameters determining the curvature and maximum value of the inverter efficiency curve.

2.3 BUILDINGS

2.3.1 Building surface identification and modeling

High-resolution LiDAR (Light Detection And Ranging) data was used to identify potential rooftops for BAPV systems in Uppsala. The total city area covered by the data is shown in Figure 3, covering 40,730 individual buildings. The software ArcGIS was used to pre-process the data into a form suitable for further calculations. By using the built-in geoprocessing tools in ArcGIS in combination with the property map of Uppsala, which represents buildings as polygons, the LiDAR data could be filtered to use only the non-ground data points within building polygons. The data were rasterized into 4 m² raster cells and for each such cell a number of parameters were calculated (tilt, azimuth, annual irradiation) to be able to filter out building areas based on their annual irradiation and to calculate hourly PV power generation. Figure 4 shows examples of the rasterized data for a small subset of the data.





Figure 3. Geographical extent of the high-resolution LiDAR data for the city of Uppsala used for identifying suitable rooftop areas in the BAPV scenarios.



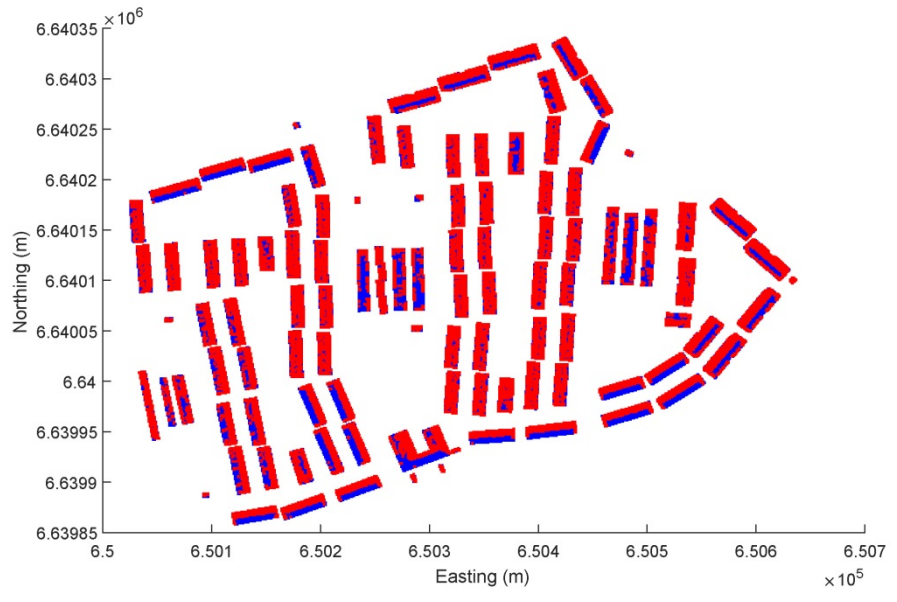


Figure 4. An example of a residential area in Uppsala aerially photographed (above) and represented by the raster based on LiDAR data (below). In the lower subfigure, red and blue cells have annual irradiance below and above 1000 kWh/m², respectively.

2.3.2 Scenarios

The municipality of Uppsala has set goals for PV installations of 30 MW installed power by 2020 and 100 MW by 2030. In 2016 the whole municipality had 4.4 MW PV installed, which means many new installations are needed over the next few years to meet the 2020 goal. The scenarios that were created within the project quantify which roof areas and fractions of buildings in the city of Uppsala need to



be used for PV installations to get total peak powers close to the goals, and how these relate to module efficiency and minimum required rooftop irradiation.

To create scenarios for future deployment of BAPV, rooftop areas were selected based on two factors: (1) an assumed fraction of buildings equipped with PV systems and (2) the areas on these buildings that have an annual solar irradiation exceeding a threshold value (to exclude unfavorably tilted or shaded areas). PV power generation from the selected rooftop areas were calculated with the PV system model above, using a representative PV module with a peak power of 260 W and an area of 1.63 m².

First, a number of scenarios were created by varying the first factor and keeping the second factor constant at 1000 kWh/m² (corresponding to what can be regarded as economically feasible over the time horizon considered). The buildings included were chosen randomly. These scenarios are listed in Table 3. Second, to check the sensitivity of the scenarios to the chosen irradiation threshold and to fine-tune the scenarios to match Uppsala municipality's 2020 and 2030 goals, the irradiance threshold was varied within scenarios 2 and 4, as shown in Table 4 and Table 5.

The scenarios closest to the goals, scenarios 2b and 4b, require that areas with annual irradiation higher than 990 kWh/m² on 17% and 50% of the buildings in the city are used for PV installations. This corresponds to total roof areas of 187 m^2 and 580 m^2 , respectively. The total roof area in the whole municipality available for PV in 2020 (accounting, e.g., for obstacles on roofs) has been estimated to 5.9 km² [22], which means that these two scenarios require that 3% and 10% of the total available roof area is used for PV installations.

Table 3. Basic scenarios based on the number of included buildings and an annual irradiation threshold of 1000 kWh/m².

Scenario	Included buildings	Total rooftop area (thousands of m²)	Installed PV power (MW)
1	1/7	136	21.7
2	1/6	168	26.8
3	1/3	331	52.8
4	1/2	494	78.7
5	4/5	819	131
6	9/10	918	146

Table 4. Scenario 2 with different annual irradiation thresholds.

Scenario	Annual irradiation threshold (kWh/m²)	Total rooftop area (thousands of m²)	Installed PV power (MW)
2a	700	299	47.8
2b	990	187	29.9
2c	1000	168	26.8
2d	1100	9.55	1.52



Table 5. Scenario 4 with different annual irradiation thresholds.

Scenario	Annual irradiation threshold (kWh/m²)	Total rooftop area (thousands of m²)	Installed PV power (MW)
4a	700	922	147
4b	990	580	92.5
4c	1000	494	78.7
4d	1100	31	4.96



3 Results

3.1 PHOTOVOLTAIC SYSTEM PERFORMANCE

Complete data covering the studied one-year period could be obtained for six of the PV systems. Average hourly performance ratio (PR) and annual specific yield are included in Table 6. The PR was calculated as the actual production divided by the theoretical yield based on the solar logger data. The values for the PR are all within a reasonable range, similar to the findings of a study of around 100 German PV systems, which showed a span of PRs between around 70% and 90%, with a median value of around 84% [17]. The specific yield of the systems is also within the expected range considering their design, for example that the façade-mounted system (Vaksala Eke) has the lowest yield. The best-performing system (Granegården) probably owes its high yield to its unshaded location and optimal tilt angle. A detailed analysis of what gives the best-performing systems their PRs and yields was not within the scope of this project but could be interesting for further study.

Table 6. System performance indicators for the PV systems for which annual data were available over the whole measurement period of the sensor network.

Site	Average performance ratio (%)	Annual specific yield (kWh/kW _p)
Granegården	88	908
Vaksala Eke (facade)	75	700
Salagatan	85	836
Geocentrum	76	774
Sala	83	839
SciencePark	90	846

3.2 MODEL FITTING AND VALIDATION

3.2.1 Correlation model

The correlation model for the instantaneous clear-sky index was fitted to sensor network data from both Hawaii (for distances < 1 km) and Uppsala (for distances > 1 km). Examples of data and fitted curves can be seen for three daily clear-sky index categories in Figure 5. At least for higher daily clear-sky index values the Hawaii and Uppsala data correspond well, in that the Uppsala data appear to show a continuation of the correlation pattern observed at Hawaii. This is an interesting finding, as it suggests that irradiance patterns are universal regardless of geographic location, given that proper normalizations (to clear-sky irradiance) and parameterizations (daily clear-sky index) are made. As hypothesized, the data suggest that the correlation decreases fast for the first kilometers and then decreases more slowly, which the correlation model is capable of capturing.



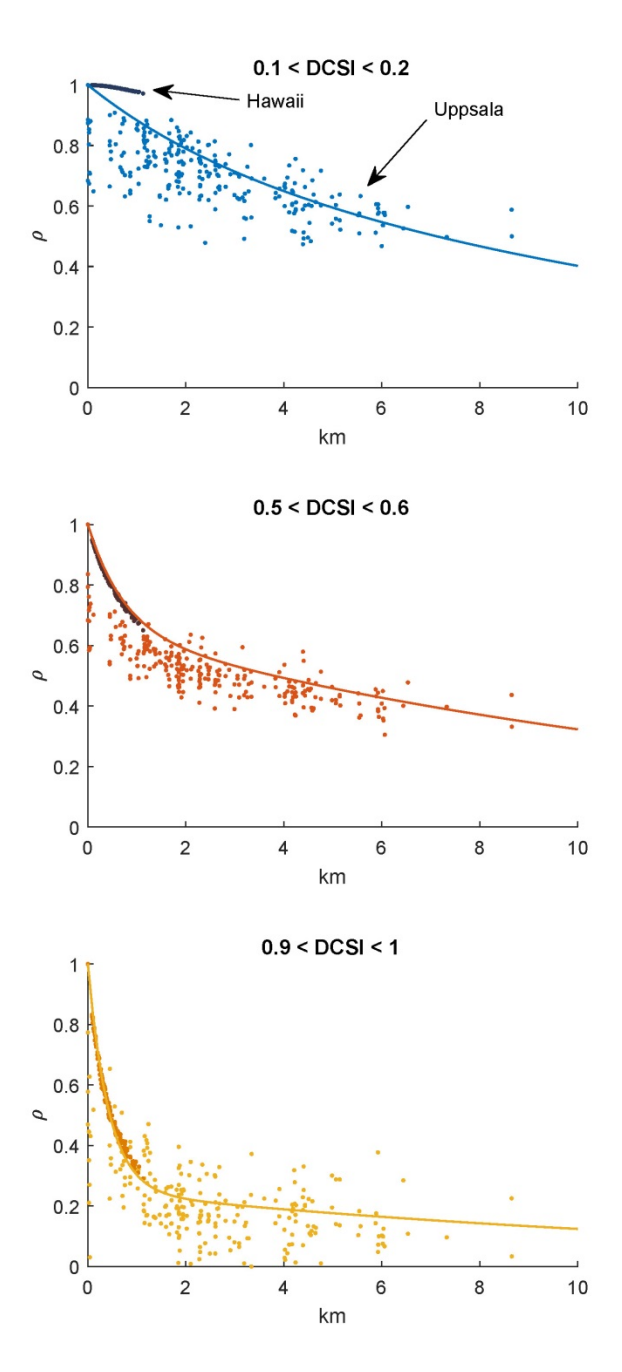


Figure 5. Correlations between sensors in the Hawaii and Uppsala networks for different daily clear-sky index (DCSI) categories, along with the model in Equation 3 fitted to the data. Every point corresponds to a pair of sensors.

A simple parameterization of the correlation function parameters was made based on model fitting in different daily clear-sky index categories. The parameters were formulated as functions of the daily clear-sky index as follows:

$$\beta(\bar{\kappa}) = \begin{cases} 0.8 & \bar{\kappa} < 0.4 \\ 1.2 - \bar{\kappa} & \bar{\kappa} \ge 0.4 \end{cases}$$
 (20)



$$\alpha_1(\bar{\kappa}) = 0.07 \text{ [km}^{-1}]$$
 (21)

$$\alpha_2(\bar{\kappa}) = 2.5\bar{\kappa} \text{ [km}^{-1}]$$
 (22)

3.2.2 Probabilistic solar irradiance model

Under the assumption that normalized solar irradiance distributions are universal, as argued above, the parameters for the probabilistic model of the instantaneous clear-sky index were determined from the Hawaii irradiance sensor data, which is more highly resolved than the Uppsala data and thus closer to instantaneous values. For the cloudy states the component proportions, mean values and standard deviations of the Gaussian mixture model were highly dependent on daily clear-sky index. As for the correlation above, simple functions were used to describe the fitted parameters in different daily clear-sky index categories, as shown in Figure 6.

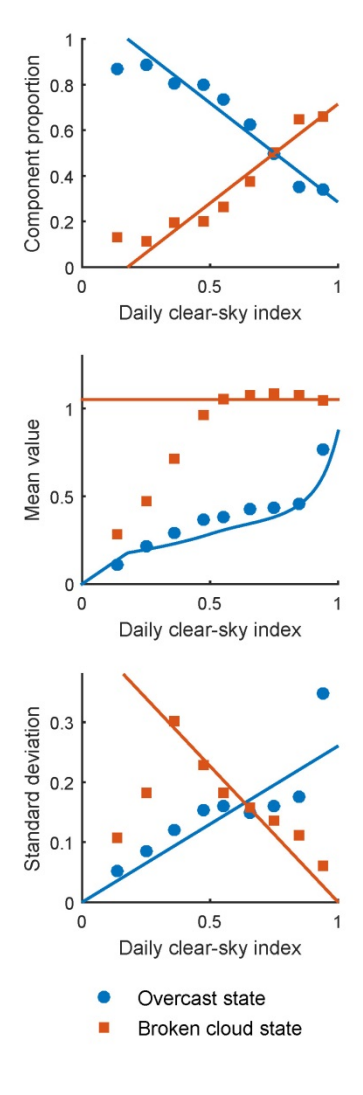


Figure 6. Fitted paramaters in the mixture Gaussian model for the cloudy states as functions of daily clear-sky index. The solid lines show the fitted functions for describing this dependence on daily clear-sky index.



The clear state distribution was found to be highly Gaussian, narrow and independent of the daily clear-sky index, with a mean value $\mu_s = 1.00$ and standard deviation $\sigma_s = 0.018$. The fraction of time with clear weather over the whole sensor network was found to have a close to quadratic dependence on the daily clear-sky index and was modeled as $s = 1.9(\bar{k} - 0.50)^2$ for values above $\bar{k} = 0.50$. For lower daily clear-sky indices, the cloudiness is too high for there to be any moments with clear skies over the whole network. Note that this should, at least to some extent, depend on the configuration and spatial extent of the network, however we assume that this function holds for the Uppsala network as well.

The probability distributions for the aggregate clear-sky index resulting from Monte Carlo simulations of the instantaneous irradiance in the Uppsala sensor network are shown in Figure 7. The copula method was used with the fitted correlation model above to get correlated samples for these simulations, and the fitted distribution models were used as marginal distributions at each site in the network. The figure also shows the empirical aggregate distributions. Evidently, the model is able to capture both the shape of the aggregate distributions and their dependence on the daily clear-sky index, suggesting that the model should be possible to use for any network configuration.

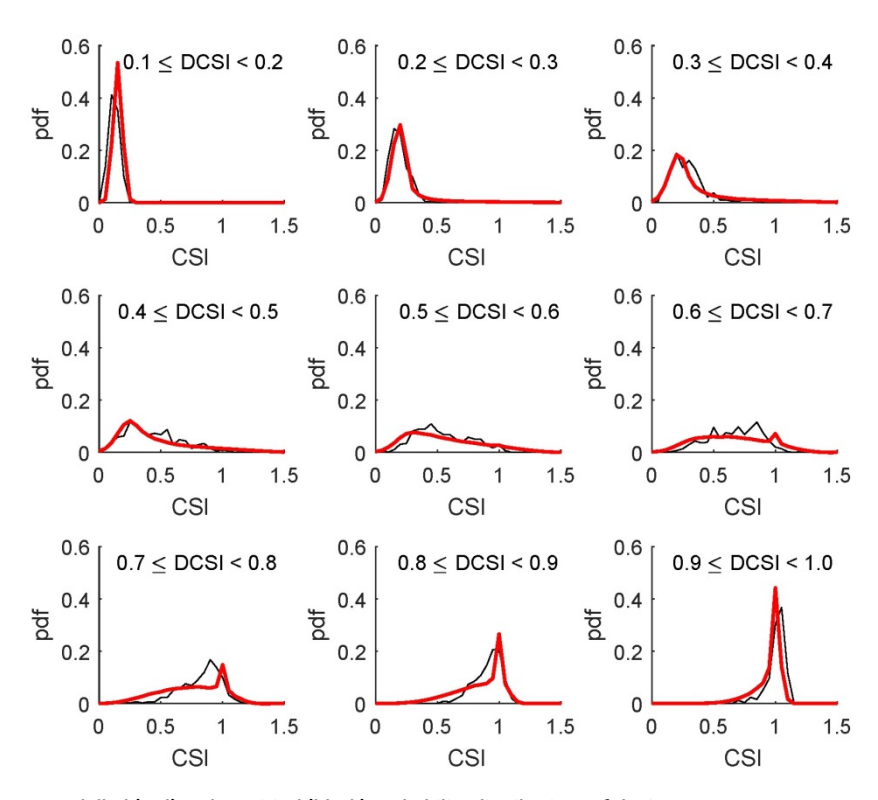


Figure 7. Modelled (red) and empirical (black) probability distributions of the instantaneous aggregate clearsky index over all sensors in the Uppsala network for different daily clear-sky index (DCSI) categories.



3.2.3 Photovoltaic system model

Six PV systems had complete data with at least an hourly time resolution during a common time period to evaluate the performance of the PV system model to reproduce aggregate solar power generation from a set of dispersed systems. For some of these systems the data could only be downloaded one day at a time, so to minimize manual work while ensuring a sufficient data for model validation a period of 268 hours with sunshine (i.e. hours with the sun above the horizon) were extracted and used for validation. The PV model was applied to the solar irradiance measured by the sensors in the plane of the PV modules with system parameters specific to each individual PV system.

The validation results can be seen in Table 7. The mean relative error is the average of the errors relative to the measured values in each hour. The normalized absolute error is the average of the absolute errors in each hour normalized by installed power. The individual systems have, in some cases, a very high error (e.g., the Ultuna system, possibly due to erroneous data or system malfunction during some hours), but when aggregated the model has a much smaller relative error, very close to the one aimed for in the project milestones. Since that aim was formulated assuming many more PV systems would have useable hourly production data, this result is still satisfying. The validation suggests that this type of PV system model, which is fairly uncomplicated and requires a minimum of component specifications, works well on aggregate power generation, already for a set of four dispersed systems.

Table 7. Performance of the PV system model for the four systems with at least hourly resolution and for their aggregate power output. The comparison was made for 268 hourly non-zero values.

System	Measured production (kWh)	Modeled production (kWh)	Mean relative error (%)	Normalized absolute error (W/W _P)
Granegården	2329	2287	13.7	3.08
Vaksala Eke (facade)	717	753	21.1	2.65
Ultuna	285	350	286	10.6
Sala	6327	6346	9.75	3.85
Aggregate	9658	9736	5.72	1.45

Modeled and measured aggregate production are also shown hour by hour during one week in Figure 8 and as a scatter plot in Figure 9, both clearly indicating the good agreement between model and measurements.



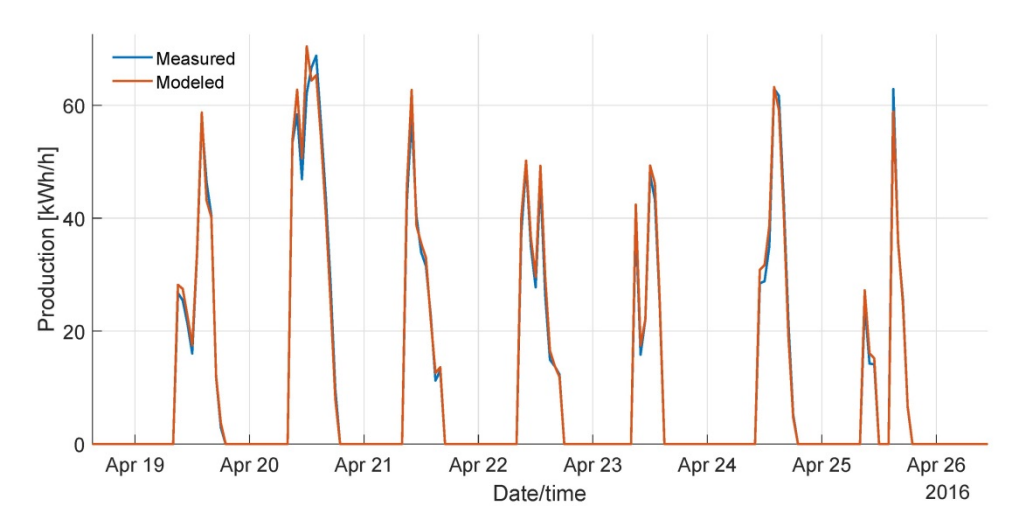


Figure 8. Measured and modeled hourly aggregate power output for the four PV systems in Table 7 for one week in April 2016.

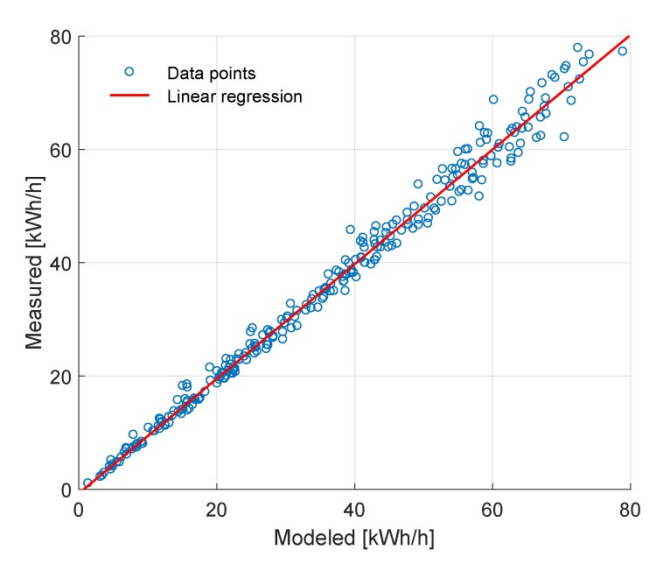


Figure 9. Agreement between 268 hourly values of measured and modeled aggregate power output for the four PV systems in Table 7.

3.3 CHARACTERIZATION OF CITY-SCALE SOLAR POWER VARIABILITY

3.3.1 Annual, seasonal and diurnal variability

Hourly data for solar power generation from BAPV systems in Uppsala in the scenarios were calculated by applying the PV system model to all included rooftop areas (corresponding approximately to 17% and 50% of the feasible rooftop areas, cf. Table 3), using the median year irradiance data for determining incident irradiance on the differently oriented BAPV systems. The resulting annual yield in the different scenarios can be seen in Figure 10. Monthly and hourly variations can be seen for the two scenarios corresponding to the city's goals in Figure 11 and Figure 12.



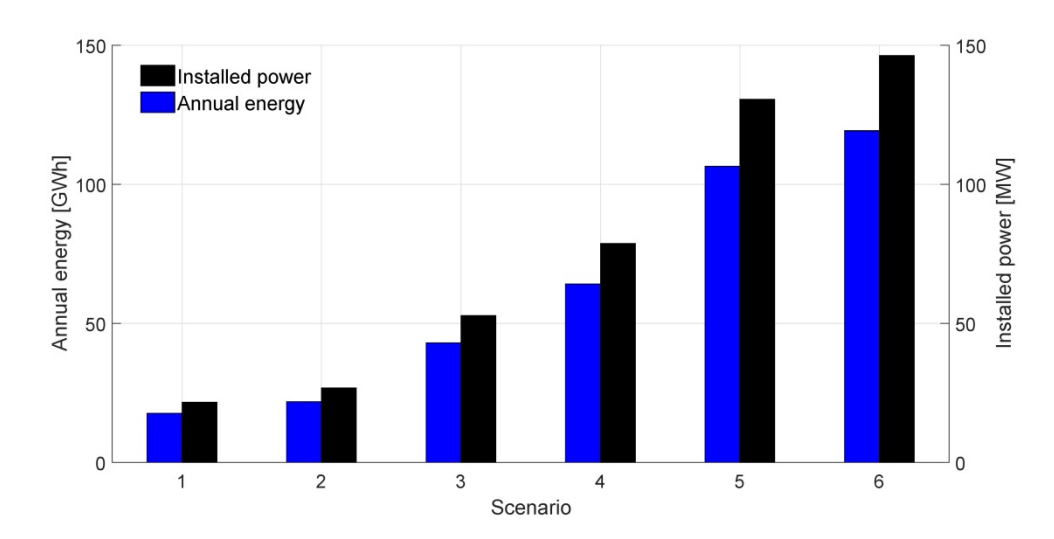


Figure 10. Calculated annual aggregate yield from city-wide BAPV in Uppsala for the different scenarios in Table 3.

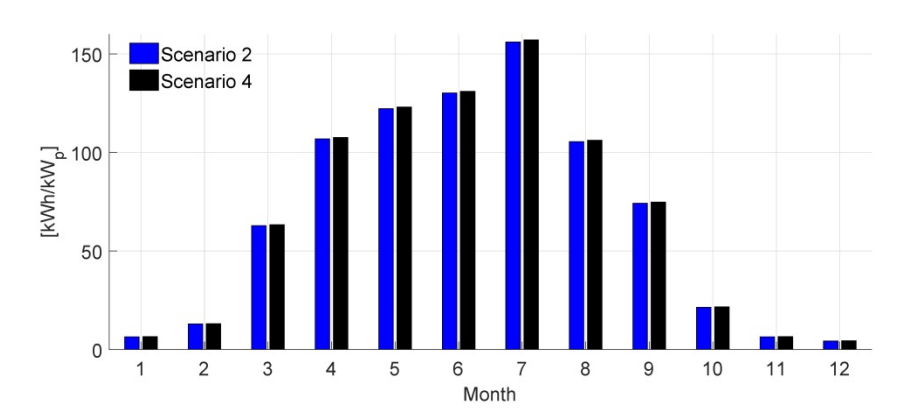


Figure 11. Monthly variation in the normalized energy yield from city-wide BAPV in Uppsala for scenarios 2 and 4 in Table 3.

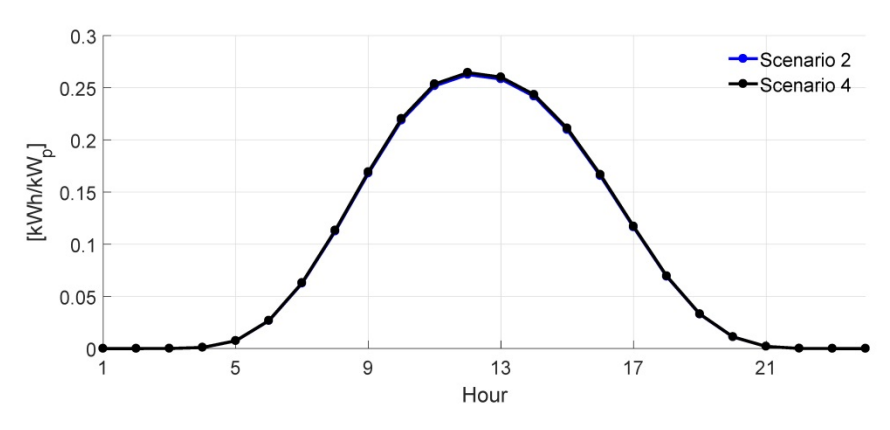


Figure 12. Average diurnal variation in normalized yield from city-wide BAPV in Uppsala for scenarios 2 and 4 in Table 3.



As can be seen in Figure 10, the annual yield in the basic scenarios 2 and 4 is 22 GWh and 64 GWh, respectively. For the fine-tuned scenarios 2b and 4b, the yield is 24 GWh and 75 GWh. The total electricity demand in Uppsala municipality around 2020-2030 has been estimated to 1500 GWh/year [23], which means that building-applied PV systems in scenarios 2b and 4b cover approximately 1.6% and 5% of the annual electricity demand.

Figure 11 and Figure 12 show that there is not much difference in the seasonal and diurnal variations between the scenarios when they are normalized to the installed power. This is because the scenarios assume no particular concentration of systems to different areas of the city or different types of buildings, thus making the distribution of systems the same between the scenarios. A comparison between different geographical dispersions would be interesting, but requires more data about the buildings to make relevant and realistic scenarios for BAPV deployment.

Note also the high yield for the month of July in Figure 11. Since the data are based on a constructed median year, this is a consistent monthly difference. A deeper investigation into the irradiance data from STRÅNG showed that the total amount of beam radiation (radiation directly from the sun, unaffected by clouds and atmospheric scattering) was highest in July compared to the other months, as determined from averages of monthly irradiance 1999-2016. This difference gets even more pronounced for tilted building-applied PV systems, for which beam radiation is scaled up more than diffuse radiation.

3.3.2 Instantaneous power generation

The smoothing effect on the instantaneous irradiance over Uppsala was determined by applying the probabilistic model for instantaneous irradiance to the building areas included in the scenarios. The buildings that were randomly chosen to be included in scenarios 2 and 4 are shown in Figure 13. Rooftops on these buildings included in scenarios 2b and 4b, i.e. having at least 990 kWh/m² of annual irradiation, are shown in Figure 14. The difference in number of included roof areas in the two scenarios can be clearly seen.

Since it is too computationally heavy to apply the copula method to all individual rooftops the total installed PV peak power was determined for each 1000×1000 m square in a grid covering the city, as also shown in Figure 14. The distances between all 54,756 pairs of grid square midpoints were determined and converted into pair-wise correlations using the correlation model fitted to the Uppsala sensor network data. A Monte Carlo simulation was then performed, in which 100,000 sets of 234 correlated clear-sky index values (one for each grid square) were sampled from the fitted clear-sky index distributions. Aggregate clear-sky index values were then determined as weighted sums over all grid squares in each of the 100,000 sets of correlated samples, with the weights equal to each square's relative share of installed PV peak power.

The result for a daily clear-sky index of 0.8, i.e. a fairly clear day, can be seen in Figure 15. Once again, there is not much difference between the scenarios because the dispersion is the same. However, there is a clear difference between the distribution of the clear-sky index over one PV system (one point location) and the



distribution of the aggregate clear-sky index over the whole city. The aggregate clear-sky index has a more Gaussian-like distribution with shorter lower and upper tails, i.e. the probabilities for both very low and very high values are lower than for a point location. For highly separated sites with site-pair correlations close to zero, the aggregate distribution will approach a single Gaussian distribution [21]

This upper-tail reduction, which is the most important result of the smoothing effect since it reduces the aggregate impact of PV systems on the distribution grid, is quantified for different daily clear-sky index values in Table 8. For all daily clear-sky indices there is a smoothing effect, but it is naturally most important for the higher daily clear-sky index values because of the very high occurrence of large values. For example, on a day with a daily clear-sky index of 0.85, the instantaneous irradiance is above that of a clear sky almost 50% of the time, due to the frequent occurrence of cloud edge effects in broken clouds (cloud edges concentrating the sunlight), an effect that is heavily reduced for the aggregate clear-sky index.



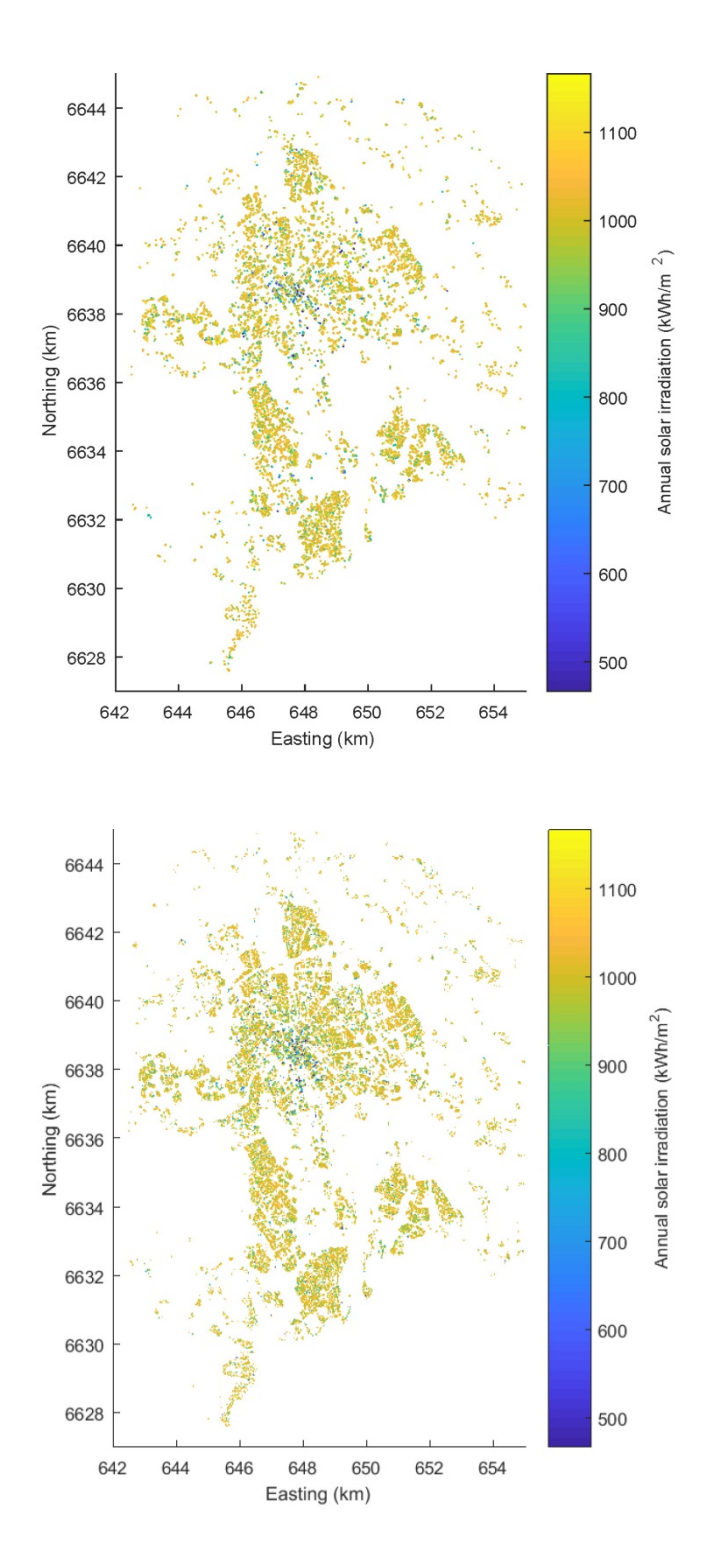


Figure 13. Selected buildings in Uppsala in scenarios 2 (top) and 4 (bottom). Colors show the annual solar irradiance on the whole rooftops.



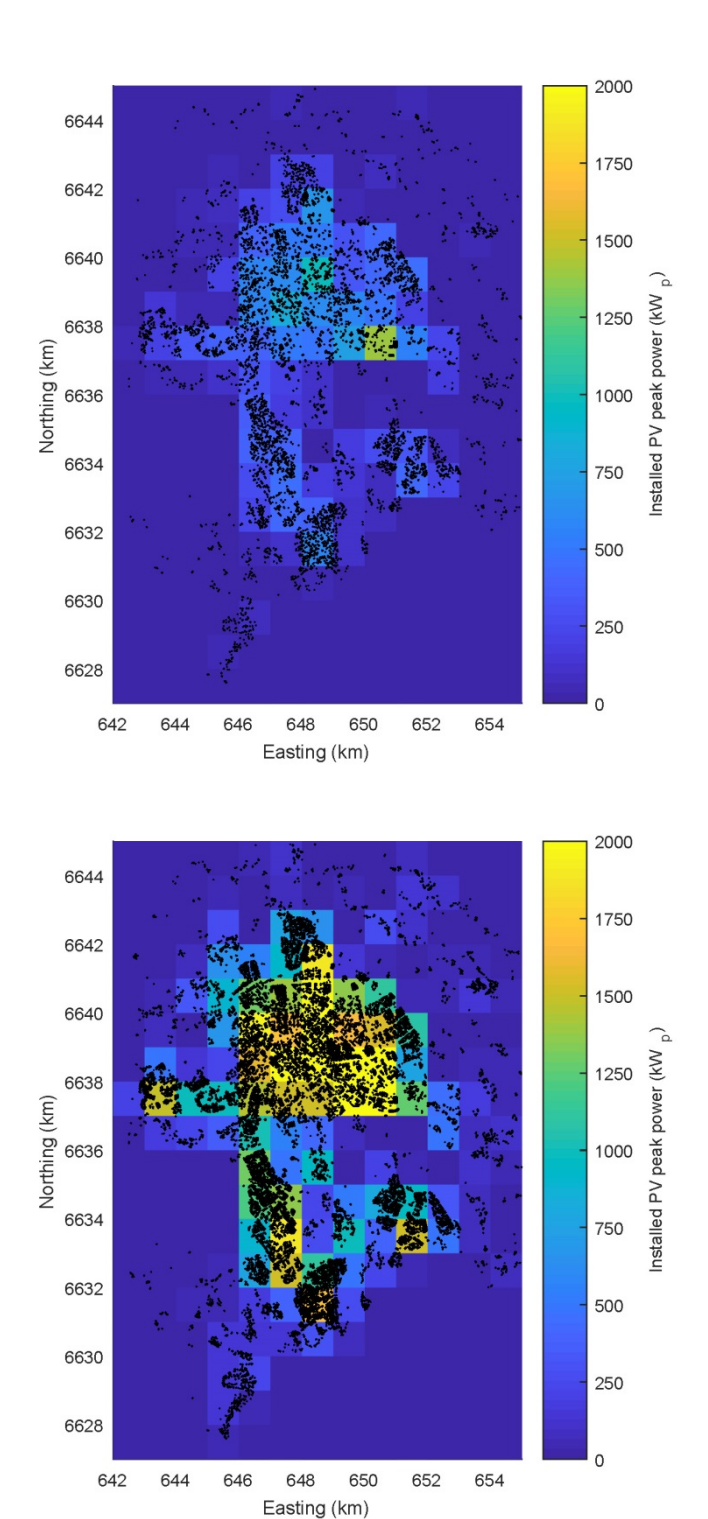


Figure 14. Included rooftop areas in Uppsala in the scenarios 2b (top) and 4b (bottom) categorized into a square grid to provide inputs to the model for instantaneous irradiance smoothing. Colors indicate the total installed PV peak power in each grid square.



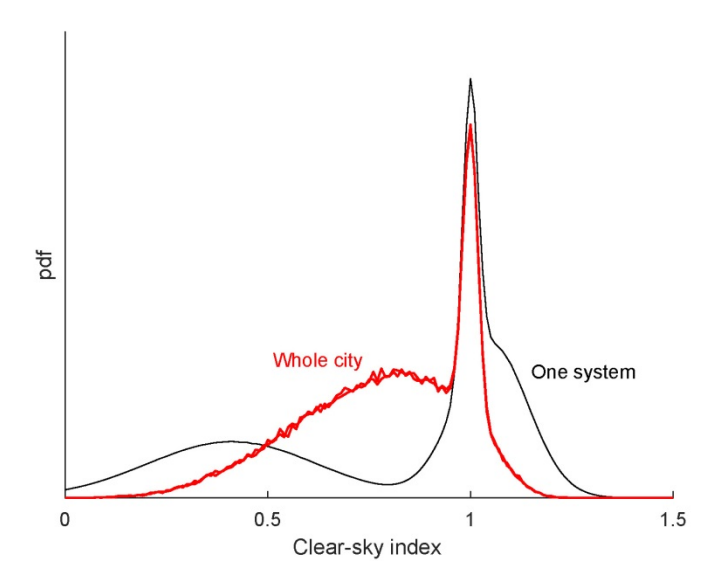


Figure 15. Resulting probability distributions for the aggregate instantaneous clear-sky index in the scenarios for Uppsala (red) compared to the probability for the instantaneous clear-sky index at one site (black).

Table 8. Resulting probabilities for high values of the clear-sky index (CSI) at one site and aggregated over the whole city of Uppsala in the scenarios.

Daily clear-sky index	Probability for CSI > 1 at one site (%)	Probability for CSI > 1 over whole city (%)
0.15	0	0
0.25	3.6	1.5
0.35	8.5	3.6
0.45	14	5.7
0.55	20	7.3
0.65	27	10
0.75	35	14
0.85	47	21
0.95	61	34

3.3.3 Intra-hourly power fluctuations

Relative variability was determined for different daily clear-sky index values by applying the method described in Section 2.1.2. The correlations are needed also for this calculation, but since the step-change correlations decay over much shorter distances than the instantaneous irradiance the grid was made finer than above, using 500×500 m grid squares. Apart from this the correlations were determined in the same way. Conversion to the time domain was done assuming a constant cloud speed of 5 m/s and a wind from the south.

The resulting relative variability for 1-second and 1-hour step-changes is shown in Table 9. The smoothing as predicted by the model is substantial for 1-second fluctuations but less so for hourly fluctuations. The variance of the changes from



one second to another in the aggregate power over the whole of Uppsala is just around 2–4% of what it would be at a single site. For hourly values, naturally, the smoothing effect is much smaller, but increases for higher daily clear-sky indices. Note, though, that these are relative values and depend on what the variance at an individual point location is. The variance for hourly values is usually smaller to start with.

It should also be noted that these figures for the step-change variability were determined using a fairly simplified model, and more elaborate models should be developed in future research.

Table 9. Resulting relative variability for step-changes in the scenarios for Uppsala.

Daily clear-sky index	Relative va	riability (%)
	1 s	1 h
0.15	4.1	55
0.25	4.0	53
0.35	3.9	51
0.45	3.7	48
0.55	3.3	41
0.65	2.9	34
0.75	2.5	28
0.85	2.1	21
0.95	1.7	15



4 Concluding discussion

This report has shown that it is possible to combine probabilistic modeling of solar irradiance and fairly simple PV system modeling to accurately characterize the aggregate solar power generation of a city. Some of the models described in the report are in the forefront of international research and this project has contributed to advance the field in a number of ways. The most important findings regarding this model development are:

- When properly normalized and parameterized, the properties of solar irradiance as determined from a sensor network such as the ones in Uppsala and Hawaii appear to be more or less universal. Results and models from this project should therefore be generally applicable for other locations as well.
- Both probability distributions for instantaneous solar irradiance and correlations in instantaneous irradiance between pairs of sites are significantly different depending on the overall cloudiness level over time, here represented by the daily clear-sky index. Using this as a parameter in the models makes them more accurate and precise.
- Monte Carlo simulations based on correlated sampling using copulas and three-state probability marginal distributions for the instantaneous solar irradiance can generate highly accurate solar irradiance data for any set of building-applied PV systems with arbitrary number of systems and dispersion.
- The PV system model used in the report, including temperature dependence and reflection losses as well as a simple linear PV array model, though being too inaccurate for individual systems, is highly accurate for aggregates of systems, with a substantial improvement in accuracy already for four aggregated dispersed PV systems.

All the milestones of the project have been reached, or very nearly reached:

- 1. The sensor network in Uppsala has collected one year of 5-min solar irradiance data from 24 solar loggers at 13 systems, and this data could be used for evaluating the performance of 6 of these installations (the limitation was in the quality of the PV power generation data monitored by the system owners). This irradiance data will be made publicly available.
- 2. The PV system model developed could be validated against the aggregate hourly power generation from four monitored PV systems. The average relative error for hourly values was 5.7% (1.5% relative to the installed power), i.e. very close to the <5% that was aimed for. However, on an even more aggregated level, it is believed to fulfill this aim.
- Mathematical models were developed, as described above, that can characterize all the properties of city-wide solar power generation that were aimed for.
- 4. Scenarios for BAPV in the city of Uppsala, corresponding closely to the 2020 and 2030 goals of the municipality were constructed and used to quantify



average daily and seasonal variations, instantaneous irradiance and fluctuations (step-changes) on different time horizons.

The usefulness and applicability of the developed models has been shown in the case study on the city of Uppsala. We have shown that by using roof areas with an annual irradiation above 990 kWh/m² on 17% and 50% of the buildings in the city, respectively, 30 MW and 93 MW installed PV capacity can be reached, close to the 2020 and 2030 goals of 30 MW and 100 MW. The roof area needed for these installations corresponds to 3% and 10% of the total available roof area in the municipality, and the annual generation from the PV systems would cover 1.6% and 5% of the estimated demand for electricity around 2020-2030.

When LiDAR data are available for identifying rooftops, as has been the case here, a very detailed mapping of the available areas for BAPV systems can be made and used as inputs to the irradiance and PV models. In particular, the simulated instantaneous irradiance and irradiance step-changes show that there is a considerable smoothing effect on the city-wide aggregate solar irradiance, substantially reducing the probability for high aggregate powers and intra-hourly power fluctuations. For example, over the whole city of Uppsala, the probability for high irradiance peaks (clear-sky index > 1) is reduced by 50-60% in most weathers compared to a single site in the studied scenarios.

The data, models and findings from the project can be used by municipalities and other organizations in their energy planning and preparation of solar roadmaps, by distribution and transmission system operators for planning and operation of power distribution and transmission networks with high shares of solar power, and not least for forecasting of solar irradiance and solar power, where the smoothing effect resulting from spatial dispersion is directly related to the accuracy of the forecast. All of these applications are interesting for future research and development.



References

- [1] J. Olauson, M.N. Ayob, M. Bergkvist, N. Carpman, V. Castellucci, A. Goude, D. Lingfors, R. Waters, J. Widén, Net load variability in Nordic countries with a highly or fully renewable power system, Nature Energy 1 (2016) 16175.
- [2] J. Widén, N. Carpman, V. Castellucci, D. Lingfors, J. Olauson, F. Remouit, M. Bergkvist, M. Grabbe, R. Waters, Variability assessment and forecasting of renewables: A review for solar, wind, wave and tidal resources, Renewable and Sustainable Energy Reviews 44 (2015) 356-375.
- [3] M. Bollen, F. Hassan, Integration of Distributed Generation in the Power System, Wiley, 2011.
- [4] M. Braun, et al., Is the distribution grid ready to accept large-scale photovoltaic deployment? State of the art, progress, and future prospects, Progress in Photovoltaics: Research and Applications 20 (2012) 681-697.
- [5] D. Lingfors, U. Zimmermann, J. Widén, Determining intra-hour solar irradiance variability with a low-cost solar logger network, Proceedings of the 4th International Workshop on Integration of Solar Power into Power Systems, Berlin, Germany, November 10-11, 2014.
- [6] HOBO Pendant® Temperature/Light 64K Data Logger, http://www.onsetcomp.com/products/data-loggers/ua-002-64 (2017-05-02).
- [7] CAMS McClear Service for estimating irradiation under clear-sky http://www.soda-pro.com/web-services/radiation/cams-mcclear (2017-05-02).
- [8] Solar Measurement Grid (1.5-Year Archive), 1-Second Global Horizontal Irradiance, Oahu, Hawaii, https://www.nrel.gov/midc/oahu_archive/ (2017-05-02).
- [9] L.M. Hinkelman, "Differences between along-wind and cross-wind solar irradiance variability on small spatial scales," Solar Energy, vol. 88, pp. 192-203, 2013.
- [10] J. Munkhammar, J. Widén, L. Hinkelman, "A copula method for simulating correlated instantaneous solar irradiance in spatial networks," Solar Energy, vol. 143, pp. 10-21, 2017.
- [11] STRÅNG a mesoscale model for solar radiation, http://strang.smhi.se/ (2017-05-02).
- [12] C.A. Glasbey, R. Graham, A.G.M. Hunter, Spatio-temporal variability of solar energy across a region: a statistical modelling approach, Solar Energy 70 (2001) 373–381.
- [13] K.G.T. Hollands, H. Suehrcke, A three-state model for the probability distribution of instantaneous solar radiation, with applications, Solar Energy 96 (2013) 103–112.
- [14] J. Widén, A model of spatially integrated solar irradiance variability based on logarithmic station-pair correlations, Solar Energy 122 (2015) 1409-1424.



- [15] D.L. King, E. E. Boyson and J. A. Kratochvil (2004). Photovoltaic Array Performance Model. Albuquerque, NM, Sandia National Laboratories, SAND2004-3535.
- [16] D.L. King, S. Gonzalez, G.M. Galbraith, and W.E. Boyson, Performance Model for Grid-Connected Photovoltaic Inverters, Sandia Report SAND2007-5036, 2007.
- [17] N.H. Reich, B. Mueller, A. Armbruster, W. G. J. H. M. van Sark, K. Kiefer, and C. Reise, Performance ratio revisited: is PR > 90% realistic?, Progress in Photovoltaics 20 (2012) 717–726.
- [18] J. Munkhammar, J. Widén, Correlation modeling of instantaneous solar irradiance with applications to solar engineering, Solar Energy 133 (2016) 14-23.
- [19] A. Ångström, On the computation of global radiation from records of sunshine, Arkiv för geofysik 5 (1956) 41–49
- [20] J.A. Duffie, W.A. Beckman, Solar Engineering of Thermal Processes (3rd ed.), Wiley, Hoboken, New Jersey, 2006.
- [21] J. Munkhammar, J. Rydén, J. Widén, D. Lingfors, Simulating dispersed photovoltaic power generation using a bimodal mixture model of the clear-sky index, Proceedings of the 30th European Photovoltaic Solar Energy Conference (EU PVSEC), Hamburg, Germany, September 14-18, 2015.
- [22] B. Sigurdson et al., Färdplan klimatneutralt Uppsala: Ett underlag för strategisk utveckling av klimatmål, samt planer och åtgärder för minskad klimatpåverkan, Uppsala kommun, 2015. Available online: http://klimatprotokollet.uppsala.se/for-studenter/klimatfardplan_uppsala/ (2017-06-15).
- [23] J. Hammam, S. Johansson, H. Persson, Potential for Solar Energy on Rooftops in the Municipality of Uppsala, Bachelor thesis, Uppsala University, 2013.



CHARACTERIZATION OF EXTENSIVE CITY-SCALE SOLAR POWER GENERATION

Grid-connected, building-applied solar power has increased rapidly worldwide over the last decades, suggesting that the cities of the future might not just be load centers but major power providers.

With large amounts of solar power in the power system, there will be challenges for both distribution and transmission system operators.

Here the solar power variability has been studied on a geographic scale of 1 to 10 km, which is the spatial extent of a medium-sized Swedish city.

The aim of the project has been to develop methodologies for quantifying the variability of aggregate solar power generation from building-applied photovoltaic systems in a city and apply these to characterize city-wide solar power generation.

Energiforsk is the Swedish Energy Research Centre – an industrially owned body dedicated to meeting the common energy challenges faced by industries, authorities and society. Our vision is to be hub of Swedish energy research and our mission is to make the world of energy smarter!

